INTERNATIONAL JOURNAL FOR NUMERICAL METHODS IN ENGINEERING
*Int. J. Numer. Meth. Engng.* **41**, 1417–1434 (1998)

# SLOPE CONSTRAINED TOPOLOGY OPTIMIZATION

JOAKIM PETERSSON[1,*] AND OLE SIGMUND[2]

[1] *Department of Mathematics, Technical University of Denmark, 2800 Lyngby, Denmark*
[2] *Department of Solid Mechanics, Technical University of Denmark, 2800 Lyngby, Denmark*

## ABSTRACT

The problem of minimum compliance topology optimization of an elastic continuum is considered. A general continuous density–energy relation is assumed, including variable thickness sheet models and artificial power laws. To ensure existence of solutions, the design set is restricted by enforcing pointwise bounds on the density slopes. A finite element discretization procedure is described, and a proof of convergence of finite element solutions to exact solutions is given, as well as numerical examples obtained by a continuation/SLP (sequential linear programming) method. The convergence proof implies that *checkerboard patterns* and other numerical anomalies will not be present, or at least, that they can be made arbitrarily weak. © 1998 John Wiley & Sons, Ltd.

KEY WORDS: topology optimization; finite elements; slope constraints

## 1. INTRODUCTION

A popular technique in topology optimization is to use a variable thickness sheet formulation and penalize intermediate design values through the use of a power law, $\rho^p$, for the design $\rho$. This procedure results in possible non-existence of solutions in the continuum problem, and numerical instabilities, such as checkerboard patterns, in the discretized problems. In case the problem lacks solutions there are two ways to go: either to relax the problem, i.e. to extend the design set or to restrict the design set. In this paper we analyse a particular choice of design set restriction which gives existence of solutions and no problems with checkerboard modes.

Topology compliance optimization of elastic continua can be performed with several choices of different design parametrizations. Three groups of such parametrizations are: Variable thickness sheet models,[1, 2] homogenization techniques with a (relative) density of material at each point,[3] and 0–1 design (material or not at each point) with a constraint on the material domain's perimeter, see Reference 4 for mathematical details and Reference 5 for numerical implementation. Sometimes, some of these techniques are also mixed.

The first category includes artificial power laws that penalize intermediate densities. In case the exponent in the power law is 1, one gets a linear model that corresponds to the physical

* Correspondence to: Joakim Petersson, Division of Mechanics, Department of Mechanical Engineering, University of Linköping, S-581 83 Linköping, Sweden. E-mail: joape@ikp.liu.se

Contract/grant sponsor: Swedish Research Council for Engineering Sciences (TFR)
Contract/grant sponsor: Technical Research Council of Denmark

CCC 0029–5981/98/081417–18$17.50

*Received 2 January 1997*
*Revised 25 June 1997*

models of variable thickness sheets, sandwich plates and also locally extremal materials in problem formulations for a free parametrization of design.[6]

In this work, we treat a general continuous relation between the energy and the design, primarily with the first group's power law in mind. Variable thickness formulations for plates lead to a power law with exponent 3, and are therefore related to the first group. The idea of introducing slope constraints on the thickness function in optimization of two-dimensional continua is not new. It was proposed in plate optimization by e.g. Niordson,[7] and existence of solutions for that problem was proved by e.g. Bendsøe.[8] The constraint on the slopes is crucial for the possibility to prove existence of solutions, and therefore plays a role similar to the perimeter constraint in 0–1 design.[4] We also mention that the introduction of the constraint (on the slope or the perimeter) has a practical meaning; it controls the maximum allowed design oscillation, or in a sense, the maximum number of holes, which in turn is governed by manufacturability constraints.

In this paper we prove the existence of optimal designs for the general continuous energy–density relation including pointwise slope constraints. The proof is along the same lines as the ones in e.g. References 8 and 9. Further, we present a Finite Element (FE) convergence proof, i.e. we establish convergence of the solutions to the discretized problems to the exact solutions. The proof of this is close to the one presented for plates in Reference 9. Important differences are that we use piecewise constant design approximation, giving practical advantages, and we allow for more general dependence between the bilinear form and the design. Finally, we also solve large-scale instances of the discretized problems to numerically illustrate the FE convergence.

The organization of the rest of the paper is as follows. First an informal preview of the considered problem and results is given in Section 2, after which we proceed with the precise mathematical description. For the reader uninterested in the proofs and mathematical details, it is possible to move directly to Section 5 after having read Section 2. If, on the other hand, the reader will go through the mathematical details, Section 2 is unnecessary.

Section 3 treats the original problem statement and establishes in Section 3.2 existence of solutions. The well-known procedure to prove existence of solutions to an optimization problem, by verifying continuity of the function and compactness of the corresponding set, is used. A crucial but rather well-known result, the compactness of the design set, is proven in Appendix I.

Section 4 deals with the FE discretization of the problem and establishes the convergence of FE solutions to exact ones for decreasing mesh size. The precise result is stated at the beginning of Section 4.2, and the proof is divided into five steps that define Sections 4.2.1–4.2.5. Sections 4.2.1 and 4.2.3 show that the FE solutions will, in subsequences, converge to a pair of elements, as the mesh size is decreased. Section 4.2.2 shows that these elements 'match' in the sense of equilibrium, and Section 4.2.5 that they are actually optimal. To show the latter, we need an auxiliary result, given in Section 4.2.4, which states that we approximate density functions properly, i.e. any exact admissible density should be possible to approximate arbitrarily well by the *discretized* admissible densities.

Section 5, finally, outlines an algorithm for the discretized problem and gives numerical examples together with comments on different behaviours.

## 2. PROBLEM PREVIEW AND RESULTS OVERVIEW

Let, as usual, the total potential energy of a linearly elastic structure be written as $\mathscr{J}(\mathbf{u},\rho)=\frac{1}{2}a_\rho(\mathbf{u},\mathbf{u})-\ell(\mathbf{u})$ in which $\rho$, the material density, is the design variable, and $\mathbf{u}$ is a kinematically

 

admissible displacement field. The variable $\rho$, which is actually a *relative* density factor taking values between zero and one, will henceforth simply be referred to as *density* or *design*. This variable enters the bilinear form, e.g. as a factor $\rho^p$ through a parametrization of stiffness as $E_{ijkl} = \rho^p E^0_{ijkl}$, where $\mathbf{E}^0$ is the stiffness tensor of a given material. The problem addressed in this paper is to minimize the work of the external loads under slope constraints on the design function:

$$\text{(MC)} \quad \begin{cases} \text{Minimize} & \ell(\mathbf{u}) \\ \rho,\ \mathbf{u} \in \mathbf{V} & \\ \text{subject to} & a_\rho(\mathbf{u},\mathbf{v}) = \ell(\mathbf{v}), \quad \text{for all } \mathbf{v} \in \mathbf{V} \\ & \underline{\rho} \leqslant \rho \leqslant 1, \quad \int_\Omega \rho \, \mathrm{d}x = V \\ & \left| \dfrac{\partial \rho}{\partial x_i} \right| \leqslant c \quad (i = 1,2) \end{cases}$$

The last constraint is the 'new' slope constraint, i.e. box constraints on the partial derivatives. In order to guarantee the existence of derivatives of the density (almost everywhere) so that the slope constraint makes sense, we need to restrict the design space to the Sobolev space of functions with essentially bounded first derivatives ($W^{1,\infty}(\Omega)$). As a consequence, the admissible design functions are enforced to be (Lipschitz) continuous.

In the special linear case, i.e. $p = 1$, the slope constraints are not needed to ensure existence of solutions. Moreover, under a stress biaxiality assumption, strong convergence in $L^p(\Omega)$ of (nine node) FE design solutions to the exact one, has recently been proven.[10]

The constraints $|\partial\rho/\partial x_i| \leqslant c$ ensure that the set of designs ($\mathscr{H}$) is compact in the space of continuous functions equipped with the sup-norm $\| \cdot \|_{0,\infty,\Omega}$. Convergence in $\| \cdot \|_{0,\infty,\Omega}$ is equivalent to uniform convergence in $\Omega$, which means that functions converge 'simultaneously and equally much' at all points in $\Omega$. Existence of solutions to (MC) follows almost directly from this compactness property and the method of proof is standard in the field of optimal control.

Let us assume that $\mathbf{u}$ is approximated with any FE known to be convergent in the equilibrium problem and $\rho$ is approximated as elementwise constant. Taking $\rho$ to be constant in each element is practical since the integration in the bilinear form can be performed with $\rho$ outside the integral sign, and consequently one arrives at the usual stiffness matrices. We hence approximate continuous functions with *dis*continuous ones, i.e. we use an *external approximation*. The slope constraints are discretized such that one enforces

$$|\rho_K - \rho_L| \leqslant ch \tag{1}$$

in which $\rho_K$ and $\rho_L$ are the values in any two adjacent elements $K$ and $L$, and $h$ is the mesh size. The constraints (1) preclude design oscillations, and it is proven that *the FE density solutions converge uniformly in* $\Omega$ *to the set of density solutions of* (*MC*) *as* $h \to 0^+$. This means that spurious checkerboard patterns, if they appear, can be made arbitrarily weak by decreasing the element size. Thus, the slope constraint not only ensures existence of solutions but also essentially checkerboard free convergence of the finite element solutions (displacements *and* density).

The finite-dimensional problem to solve has the standard matrix-vector form appearing in variable thickness design with penalization, but with the linear constraints (1) added to it. The nested formulation, i.e. the problem in design variables solely, has only linear constraints, and is therefore

 

well suited for an SLP scheme. The design of the so-called MBB-beam is considered, and the problem is solved for a series of decreasing mesh sizes to illustrate the convergence, and for different $c$-values to illustrate their influence on the optimal design. The numerical results are similar to those obtained by the perimeter[5] and filtering[11, 12] techniques. As opposed to filtering techniques, the present method is mathematically well founded, but the computational time is much longer due to the large number of constraints in (1). The constant $c$, which in fact is fairly easy to choose, plays a role similar to the perimeter constraint. A large value allows for a larger number of 'bars', and a very low one yields a small number of wide 'bars' (however with grey zones). As a practical rule for how to choose $h$ and $c$, it is concluded that $hc$ should be less than $1/3$ to guarantee a design of reasonable quality free of checkerboard patterns.

## 3. THE ORIGINAL PROBLEM STATEMENT

### 3.1. Preliminaires

Let $\Omega \subset \mathbb{R}^2$ be a Lipschitz domain containing the region of the elastic body. At each point of the boundary $\partial\Omega$, and in each of two orthogonal directions, there are either prescribed zero displacements or tractions.

We introduce the usual Sobolev spaces $W^{m,p}(\Omega)$, $m \geqslant 0$, $1 \leqslant p \leqslant \infty$, and denote (any of) the usual norms and seminorms by $\|\cdot\|_{m,p,\Omega}$ and $|\cdot|_{m,p,\Omega}$, respectively, cf. Reference 13. For $p=2$ we write $H^m(\Omega) = W^{m,2}(\Omega)$, $\mathbf{H}^m(\Omega) = (H^m(\Omega))^2$, and for $m=0$ we naturally write $L^p(\Omega) = W^{0,p}(\Omega)$. We abbreviate $\|\cdot\|_m = \|\cdot\|_{m,2,\Omega}$, $|\cdot|_m = |\cdot|_{m,2,\Omega}$ and also use the same notation for the corresponding (semi)norms in $(W^{m,p}(\Omega))^2$. Further, $C^k(\overline{\Omega})$ denotes the space of $k$ times continuously differentiable functions on $\Omega$ in which all derivatives possess continuous extensions to $\overline{\Omega}$, $C^\infty(\overline{\Omega}) = \bigcap_{k=0}^{\infty} C^k(\overline{\Omega})$, and $\mathbf{C}^\infty(\overline{\Omega}) = (C^\infty(\overline{\Omega}))^2$. The set of test functions on $\Omega$, i.e. infinitely differentiable functions with compact support in $\Omega$, is denoted by $\mathscr{D}$.

The set of kinematically admissible displacements, $\mathbf{V}$, is assumed to be a closed subspace of $\mathbf{H}^1(\Omega)$, and such that (3) holds, e.g.

$$\mathbf{V} = \{\mathbf{v} \in \mathbf{H}^1(\Omega) \mid v_i = 0 \text{ on } \Gamma_u \ (i=1,2)\}$$

in which $\Gamma_u$ is the part of $\partial\Omega$ with zero-prescribed displacements.

The design variable, $\rho$, will be referred to as either *density* or *design*, and it will be restricted to belong to a set $\mathscr{H}$ of admissible designs. (In the following, $\int$ will be used in the meaning of $\int_\Omega$, and d$x$ is omitted unless the notation has a special relevance.)

$$\mathscr{H} = \left\{ \rho \in W^{1,\infty}(\Omega) \;\middle|\; \underline{\rho} \leqslant \rho \leqslant 1, \quad \left|\frac{\partial \rho}{\partial x_i}\right| \leqslant c \ (i=1,2) \quad \text{a.e. in } \Omega, \quad \int \rho = V \right\}$$

This definition is like the usual set of admissible designs in variable thickness sheet problems, i.e. the set

$$\mathscr{H}_0 = \left\{ \rho \in L^\infty(\Omega) \;\middle|\; \underline{\rho} \leqslant \rho \leqslant 1 \quad \text{a.e. in } \Omega, \quad \int \rho = V \right\}$$

but in addition to $\rho$ itself, the first-order derivatives are also restricted to $L^\infty(\Omega)$ and subject to pointwise bounds. The set $\mathscr{H}_0$ includes both the exact admissible designs and the set of discretized densities to be defined in Section 4.

 

For fixed $\rho \in \mathscr{H}_0$, we denote by $a_\rho(\cdot,\cdot)$ the internal work symmetric bilinear form on $\mathbf{V} \times \mathbf{V}$:

$$a_\rho(\mathbf{u},\mathbf{v}) = \int \eta(\rho) \frac{\partial u_i}{\partial x_j} E_{ijkl} \frac{\partial v_k}{\partial x_l}$$

in which the summation convention is used, i.e. a summation from 1 to 2 over all repeated indices is understood. Here $E_{ijkl}$ denotes, at least up to a scaling, elasticity constants satisfying the usual symmetry, ellipticity and boundedness features, and $\eta(\cdot)$ is any continuous function defined on $[\underline{\rho}, 1]$ and whose values are contained in $[\varepsilon, 1]$ for some $\varepsilon > 0$. A common choice is $\eta(\rho) = \rho^p$ for some positive real number $p$. For $p = 1$ one retains the linear variable thickness sheet model, which also models locally extremal materials and sandwich type plates, etc.

We have the following bicontinuity feature:

$$|a_\rho(\mathbf{u},\mathbf{v})| \leqslant M \|\mathbf{u}\|_1 \|\mathbf{v}\|_1, \quad \forall \mathbf{u},\mathbf{v} \in \mathbf{V},\ \forall \rho \in \mathscr{H}_0 \tag{2}$$

since the values of $\eta$ are bounded from above, and, moreover, uniform ellipticity:

$$a_\rho(\mathbf{u},\mathbf{u}) \geqslant \alpha \|\mathbf{u}\|_1^2, \quad \forall \mathbf{u} \in \mathbf{V},\ \forall \rho \in \mathscr{H}_0 \tag{3}$$

if there are 'sufficiently many' zero-prescribed displacements, and since the values of $\eta$ are bounded from below by $\varepsilon > 0$ ($\alpha$ and $M$ are strictly positive constants).

The external load linear form $\ell(\cdot)$ maps $\mathbf{V}$ into $\mathbb{R}$ and is assumed to satisfy the following boundedness feature:

$$\|\ell\| = \sup_{\mathbf{0} \neq \mathbf{v} \in \mathbf{V}} \frac{|\ell(\mathbf{v})|}{\|\mathbf{v}\|_1} < +\infty \tag{4}$$

For instance, it can take the form

$$\ell(\mathbf{v}) = \int_{\Gamma_t} \mathbf{t} \cdot \mathbf{v}\, \mathrm{d}s + \int_\Omega \mathbf{b} \cdot \mathbf{v}\, \mathrm{d}x$$

where $\mathbf{t}$ is the given line load on $\Gamma_t$ and $\mathbf{b}$ is the given area load on $\Omega$.

From the linear and bilinear form we can define, as usual, the total potential energy as

$$\mathscr{J}(\mathbf{u},\rho) = \tfrac{1}{2} a_\rho(\mathbf{u},\mathbf{u}) - \ell(\mathbf{u})$$

for a given displacement field $\mathbf{u}$ in the body with density distribution $\rho$.

We reformulate the *minimum compliance* problem in the following form of simultaneous analysis and design:

$$\text{(MC)} \begin{cases} \text{Find } (\mathbf{u}^*, \rho^*) \in \mathbf{V} \times \mathscr{H} \text{ such that} \\ a_{\rho^*}(\mathbf{u}^*, \mathbf{v}) = \ell(\mathbf{v}), \quad \forall \mathbf{v} \in \mathbf{V}, \text{ and} \\ \ell(\mathbf{u}^*) \leqslant \ell(\mathbf{u}) \\ \text{for all } (\mathbf{u},\rho) \in \mathbf{V} \times \mathscr{H} \text{ satisfying} \\ a_\rho(\mathbf{u},\mathbf{v}) = \ell(\mathbf{v}), \quad \forall \mathbf{v} \in \mathbf{V} \end{cases}$$

Here,

$$a_\rho(\mathbf{u},\mathbf{v}) = \ell(\mathbf{v}), \quad \forall \mathbf{v} \in \mathbf{V} \tag{5}$$

 

is the variational equation for equilibrium for the structure with density $\rho$, and it is equivalent to a minimum of total potential energy:

$$\mathscr{J}(\mathbf{u},\rho)\leqslant\mathscr{J}(\mathbf{v},\rho),\quad \forall\mathbf{v}\in\mathbf{V} \tag{6}$$

By (2)–(4), there exists a unique solution $\mathbf{u}\in\mathbf{V}$ to (6) (or (5)) for any $\rho\in\mathscr{H}_0$.

We define an *admissible pair* in (MC) as any pair $(\mathbf{u},\rho)\in\mathbf{V}\times\mathscr{H}$ satisfying (5). The condition $\rho\in\mathscr{H}$ corresponds to *design constraints* and (5) to the *equilibrium constraint*.

### 3.2. Existence of solutions

The proof of existence of solutions is standard in optimal control. References 9 and 8 are very close to the presentation below.

As in e.g. Reference 14, p. 62, we only have to check that the set

$$\mathbf{U}^*=\{\mathbf{u}\in\mathbf{V}\mid\exists\rho\in\mathscr{H}: a_\rho(\mathbf{u},\mathbf{v})=\ell(\mathbf{v}),\quad\forall\mathbf{v}\in\mathbf{V}\}$$

is weakly closed, since $\ell(\cdot)$ is weakly continuous and $\mathbf{U}^*$ is weakly precompact. Hence, let $\mathbf{u}_m\in\mathbf{U}^*$ be such that

$$\mathbf{u}_m\to\mathbf{u}\in\mathbf{V}\quad\text{weakly as } m\to\infty \tag{7}$$

and let $\rho_m\in\mathscr{H}$ denote the corresponding design sequence in the definition of $\mathbf{U}^*$. We will show that $\mathbf{u}\in\mathbf{U}^*$. From the appendix we conclude that, for some subsequence and some $\rho\in\mathscr{H}$,

$$\rho_m\to\rho\quad\text{uniformly in }\Omega\text{ as } m\to\infty \tag{8}$$

Since $\eta$ is *uniformly* continuous, due to the compactness of the interval $[\underline{\rho},1]$, (8) yields

$$\eta\circ\rho_m\to\eta\circ\rho\quad\text{uniformly in }\Omega\text{ as } m\to\infty \tag{9}$$

We have, for arbitrary fixed $\mathbf{v}\in\mathbf{V}$,

$$a_{\rho_m}(\mathbf{u}_m,\mathbf{v})=\ell(\mathbf{v}) \tag{10}$$

Moreover, (7) and (9) are sufficient for

$$\lim_{m\to\infty}a_{\rho_m}(\mathbf{u}_m,\mathbf{v})=a_\rho(\mathbf{u},\mathbf{v})$$

in which $\mathbf{v}\in\mathbf{V}$ is arbitrary, and hence (10) shows that $\mathbf{u}$ is the equilibrium displacement for $\rho$. We conclude that $\mathbf{U}^*$ is weakly closed, and the proof of existence of solutions to (MC) is hereby complete.

## 4. FINITE ELEMENT APPROXIMATION AND CONVERGENCE

We choose piecewise constant and discontinuous approximation of the design variable. This may seem unnatural since the admissible designs are restricted to be continuous. However, the motivation for this choice is that constant $\rho$ results in a discretized optimization problem which can be given a simple matrix formulation with the usual stiffness matrices. In case one, for instance, uses bilinear and continuous design approximation, one has to perform new integrations to get the matrix entries, and the overall computational time would be much higher without substantially improving the design description.

 

### 4.1. Preliminaires

From now on we assume that we partition a *rectangular* domain $\Omega$ into a mesh of $m = n_x n_y$ squares of *equal size*, i.e. $n_x$ finite elements in the horizontal direction and $n_y$ in the vertical. These quite severe restrictions are made only to simplify the presentation of the mathematical manipulations. The results can be expected for much more general situations. The (open) squares are denoted $\Omega_{jk}$, and they are mutually disjoint. Moreover,

$$\overline{\Omega} = \bigcup_{j=1}^{n_x} \bigcup_{k=1}^{n_y} \overline{\Omega}_{jk}$$

If $h$ denotes the mesh size, i.e. the edge length of any square, then, clearly,

$$h^2 = |\Omega_{jk}| = |\Omega|/m$$

Henceforth, '$\forall j,k$' will mean 'for all $(j,k) \in \{1,\ldots,n_x\} \times \{1,\ldots,n_y\}$'. We define the discretized space of displacements as

$$\mathbf{V}_h = \{\mathbf{v} |\ v_i \in C^0(\overline{\Omega}), v_i|_{\Omega_{jk}} \in P_1(\Omega_{jk}) \quad \forall j,k\ (i=1,2)\} \cap \mathbf{V}$$

Here $P_\ell(\Omega)$ denotes the space of bilinear functions on $\Omega$ for $\ell = 1$, and constant functions on $\Omega$ for $\ell = 0$. From the standard theory of Sobolev spaces, we have that the space $\mathbf{C}^\infty(\overline{\Omega}) \cap \mathbf{V}$ is dense in $\mathbf{V}$, and, on this set of continuous functions one can apply the usual piecewise bilinear interpolation operator $\pi_h$ (on both components). The standard interpolation estimate[15]

$$\|\mathbf{u} - \pi_h \mathbf{u}\|_1 \leqslant Ch|\mathbf{u}|_2$$

clearly implies

$$\pi_h \mathbf{u} \to \mathbf{u}, \quad \text{strongly in } \mathbf{V}, \text{ as } h \to 0^+, \quad \forall \mathbf{u} \in \mathbf{C}^\infty(\overline{\Omega}) \cap \mathbf{V} \tag{11}$$

We will enforce the following design oscillation restrictions:

$$|\rho_{j+1,k} - \rho_{jk}| \leqslant ch, \quad j = 1,\ldots,n_x - 1, \quad k = 1,\ldots,n_y \tag{12}$$

and

$$|\rho_{j,k+1} - \rho_{jk}| \leqslant ch, \quad j = 1,\ldots,n_x, \quad k = 1,\ldots,n_y - 1 \tag{13}$$

in which $\rho_{jk}$ denotes the value in $\Omega_{jk}$ of any elementwise constant function $\rho$. We define the discretized set of densities as

$$\mathscr{H}_h = \left\{ \rho \;\middle|\; \rho|_{\Omega_{jk}} \in P_0(\Omega_{jk})\ \forall j,k, \int \rho = V,\ \underline{\rho} \leqslant \rho \leqslant 1 \quad \text{a.e. in } \Omega,\ (12) \text{ and } (13) \right\}$$

Clearly $\mathbf{V}_h \subset \mathbf{V}$, but $\mathscr{H}_h \not\subset \mathscr{H}$, which in words means that we use an *internal* or *conforming* approximation for displacements, but an *external approximation* for densities. However, $\mathscr{H}_h \subset \mathscr{H}_0$.

We now formulate the FE discretized finite-dimensional problem to solve in practice. This is merely the problem (MC) with $\mathbf{V}$ replaced by $\mathbf{V}_h$ and $\mathscr{H}$ by $\mathscr{H}_h$.

 

The *discretized* minimum compliance problem $(\mathrm{MC})_h$ is defined as

$$(\mathrm{MC})_h \begin{cases} \text{Find } (\mathbf{u}_h^*, \rho_h^*) \in \mathbf{V}_h \times \mathscr{H}_h \text{ such that} \\ a_{\rho_h^*}(\mathbf{u}_h^*, \mathbf{v}_h) = \ell(\mathbf{v}_h), \quad \forall \mathbf{v}_h \in \mathbf{V}_h, \text{ and} \\ \ell(\mathbf{u}_h^*) \leqslant \ell(\mathbf{u}_h) \\ \text{for all } (\mathbf{u}_h, \rho_h) \in \mathbf{V}_h \times \mathscr{H}_h \text{ satisfying} \\ a_{\rho_h}(\mathbf{u}_h, \mathbf{v}_h) = \ell(\mathbf{v}_h), \quad \forall \mathbf{v}_h \in \mathbf{V}_h \end{cases}$$

It is straightforward to establish existence of solutions to $(\mathrm{MC})_h$, and the existence of a unique equilibrium displacement $\mathbf{u}_h$ for any fixed $\rho_h \in \mathscr{H}_h$, i.e.

$$a_{\rho_h}(\mathbf{u}_h, \mathbf{v}_h) = \ell(\mathbf{v}_h), \quad \forall \mathbf{v}_h \in \mathbf{V}_h \tag{14}$$

Given any $h > 0$, a pair $(\mathbf{u}_h, \rho_h) \in \mathbf{V}_h \times \mathscr{H}_h$ satisfying (14) is called an *admissible pair* in $(\mathrm{MC})_h$.

### 4.2. Convergence of FE solutions

In this section we will prove that, vaguely speaking, the solutions to $(\mathrm{MC})_h$ converge to those of (MC) as $h \to 0^+$. More precisely:

*For* any *sequence of FE solutions* $(\mathbf{u}_h^*, \rho_h^*)$ *to* $(MC)_h$, *there are two elements* $\mathbf{u}^* \in \mathbf{V}$ *and* $\rho^* \in \mathscr{H}$, *and a subsequence* (*denoted again by the same symbol*) *such that* $\mathbf{u}_h^*$ *converges strongly to* $\mathbf{u}^*$ *in* $\mathbf{V}$ *and* $\rho_h^*$ *converges to* $\rho^*$ *uniformly in* $\Omega$, *as* $h \to 0^+$. *Moreover*, *any such pair of cluster points* $(\mathbf{u}^*, \rho^*)$ *solves the problem* (*MC*).

Since any sequence of FE solutions has a convergent subsequence and the limit is optimal, a sequence of FE solutions necessarily converges to the *set* of exact solutions. Hence, if the exact solution is unique, *the whole* sequence converges. An important consequence is also that, as one refines the mesh, one will necessarily come as close as one wants, measured in $\|\cdot\|_{0,\infty,\Omega}$, to an optimal density, but, two consecutive discrete solutions for different meshes might approximate two *different* true solutions.

The arguments of proof are divided into a number of steps of partial results, and the subsections next are divided accordingly. The partial results are:

1. Any sequence of FE solutions has a (weakly) convergent subsequence as $h \to 0^+$ with some limit elements.
2. Any such limit elements are coupled via equilibrium, i.e. (5).
3. The displacement sequence converges strongly.
4. The sets of approximated designs are 'close to' the original design set.
5. Any limit elements in 1 solve the problem (MC).

*4.2.1. Convergent subsequences.* From now on, let $(\mathbf{u}_h, \rho_h)$ be any admissible pair in $(\mathrm{MC})_h$ as $h \to 0^+$. In this subsection we will show that there is a subsequence which converges in the sense of (17).

From (3) and (4) one gets

$$\|\mathbf{u}_h\|_1 \leqslant \|\ell\|/\alpha$$

 

by choosing $\mathbf{v}_h = \mathbf{u}_h$ in (14). Hence, there is a weakly convergent subsequence, denoted by $\{\mathbf{u}_h\}$, with limit $\mathbf{u}$ in $\mathbf{V}$. We now show the corresponding result for the density variable.

Since the $\rho_h$'s are external approximations, we cannot immediately use the compactness of $\mathscr{H}$ to get a convergent subsequence of $\{\rho_h\}$. Instead, we create an auxiliary sequence of continuous functions, $\{\pi_L\rho_h\}$, which lies in a compact set and which is 'close to' $\{\rho_h\}$. It then follows, by compactness, that the auxiliary sequence converges to a limit, and by the 'short distance' between $\{\rho_h\}$ and $\{\pi_L\rho_h\}$, that also $\{\rho_h\}$ converges to this limit.

Let $\mathscr{S}$ be the 'surrounding strip' of width $h$ to $\Omega$, i.e. the union of all $2(n_x + n_y + 2)$ squares lying immediately outside $\partial\Omega$ (the squares are only translates of the $\Omega_{jk}$'s). Extend $\rho_h$ to $\Omega \cup \mathscr{S}$ by letting the values in squares in $\mathscr{S}$ be the ones attained in the closest $\Omega_{jk}$ in $\Omega$, and denote the extended squarewise constant function by $\rho_h$ again. Then, let $\pi_L\rho_h$ denote the *continuous* piecewise bilinear interpolation of $\rho_h$, in which the pieces now are the squares with corners in the midpoints of the $\Omega_{jk}$'s and the squares in $\mathscr{S}$, i.e. $(\pi_L\rho_h)(\mathbf{x}) = \rho_h(\mathbf{x})$ for all midpoints $\mathbf{x}$ of $\Omega_{jk}$'s or squares in $\mathscr{S}$. It then follows that

$$\left|\frac{\partial \pi_L\rho_h}{\partial x_i}\right| \leqslant c$$

almost everywhere in $\Omega$ for $i = 1, 2$, since the maximum absolute value of derivatives (almost everywhere) for a bilinear function are attained on the edges of the squares and (12) and (13) hold, and

$$\underline{\rho} \leqslant \pi_L\rho_h \leqslant 1$$

almost everywhere in $\Omega$, since the extreme function values are attained at the square corners. With the same arguments as those used in the appendix to conclude the compactness of $\mathscr{H}$, we obtain, at least for a subsequence,

$$\pi_L\rho_h \to \rho, \quad \text{uniformly in } \Omega \tag{15}$$

in which $\rho$ satisfies

$$\rho \in W^{1,\infty}(\Omega), \quad \underline{\rho} \leqslant \rho \leqslant 1, \quad \left|\frac{\partial \rho}{\partial x_i}\right| \leqslant c, \quad \text{a.e. in } \Omega \tag{16}$$

Obviously, for any $\mathbf{x}$ in $\Omega$,

$$|(\pi_L\rho_h - \rho_h)(\mathbf{x})| \leqslant ch$$

which with (15) and the triangle inequality gives

$$\rho_h \to \rho, \quad \text{uniformly in } \Omega$$

This, in turn, gives that $\int \rho = V$ since $\int \rho_h = V$. In addition we have (16), so $\rho \in \mathscr{H}$.

In conclusion, as $h \to 0^+$, there is a subsequence of any given sequence of admissible pairs in $(\mathrm{MC})_h$, that satisfy

$$\mathbf{u}_h \to \mathbf{u} \quad \text{weakly in } \mathbf{V}, \quad \rho_h \to \rho \in \mathscr{H} \quad \text{uniformly in } \Omega \tag{17}$$

In particular, the *solutions* to $(\mathrm{MC})_h$ satisfy

$$\mathbf{u}_h^* \to \mathbf{u}^* \quad \text{weakly in } \mathbf{V}, \quad \rho_h^* \to \rho^* \in \mathscr{H} \quad \text{uniformly in } \Omega \tag{18}$$

for some elements $\mathbf{u}^*$ and $\rho^*$, and some subsequence.

 

*4.2.2. Equilibrium coupling for a pair of cluster points.* We like to show that an arbitrary pair of clusterpoints $(\mathbf{u}, \rho)$ as in (17) are coupled through equilibrium, i.e. for given arbitrary $\mathbf{v} \in \mathbf{V}$,

$$a_\rho(\mathbf{u}, \mathbf{v}) = \ell(\mathbf{v}) \tag{19}$$

It follows from the density of $\mathbf{C}^\infty(\overline{\Omega}) \cap \mathbf{V}$ in $\mathbf{V}$ and (11) that there exists a sequence $\mathbf{v}_h \in \mathbf{V}_h$ such that $\mathbf{v}_h \to \mathbf{v}$. From (14) we get

$$a_{\rho_h}(\mathbf{u}_h, \mathbf{v}_h - \mathbf{v}) + a_{\rho_h}(\mathbf{u}_h, \mathbf{v}) = \ell(\mathbf{v}_h) \tag{20}$$

The first term of the left-hand side in (20) converges to zero since $\mathbf{v}_h \to \mathbf{v}$, and $\{\eta \circ \rho_h\}$ and $\{\mathbf{u}_h\}$ are bounded in $L^\infty(\Omega)$ and $\mathbf{V}$. The second term of the left-hand side converges to $a_\rho(\mathbf{u}, \mathbf{v})$, since $\eta \circ \rho_h$ converges uniformly in $\Omega$ and $\mathbf{u}_h$ weakly in $\mathbf{V}$. Hence, passing to the limit in (20), one arrives at (19).

*4.2.3. Strong convergence of displacements.* We have obtained that the FE displacement solutions converge weakly (for subsequences) as the mesh is refined. Knowing, from the previous subsection, that the limit pair is coupled through equilibrium, we can show that the displacement sequence converges strongly.

From the uniform ellipticity we have

$$\begin{aligned} \alpha \|\mathbf{u}_h^* - \mathbf{u}^*\|_1^2 &\leqslant a_{\rho_h^*}(\mathbf{u}_h^* - \mathbf{u}^*, \mathbf{u}_h^* - \mathbf{u}^*) \\ &= a_{\rho_h^*}(\mathbf{u}_h^* - \mathbf{u}^*, -\mathbf{u}^*) + a_{\rho_h^*}(\mathbf{u}_h^*, \mathbf{u}_h^*) - a_{\rho_h^*}(\mathbf{u}^*, \mathbf{u}_h^*) \\ &= a_{\rho_h^*}(\mathbf{u}_h^* - \mathbf{u}^*, -\mathbf{u}^*) + \ell(\mathbf{u}_h^*) - a_{\rho_h^*}(\mathbf{u}^*, \mathbf{u}_h^*) \end{aligned} \tag{21}$$

in which we have used (14). The first term in (21) converges to zero and the second to $\ell(\mathbf{u}^*)$. The third one, $a_{\rho_h^*}(\mathbf{u}^*, \mathbf{u}_h^*)$, converges to $a_{\rho^*}(\mathbf{u}^*, \mathbf{u}^*)$, which, in turn, equals $\ell(\mathbf{u}^*)$ by (19). Hence, from (21) we conclude

$$\mathbf{u}_h^* \to \mathbf{u}^* \quad \text{strongly in } \mathbf{V} \tag{22}$$

if only (18) holds.

*4.2.4. A density argument for designs.* As always in FE approximation theory, one must establish that any variable can be sufficiently well approximated (measured in some topology) by the discretized version of the variable. For the displacement, this was ensured by (11) and the density of $\mathbf{C}^\infty(\overline{\Omega}) \cap \mathbf{V}$ in $\mathbf{V}$. We now show that any $\rho \in \mathscr{H}$ can be approximated by $\rho_h \in \mathscr{H}_h$ arbitrarily well measured in $\|\cdot\|_{0,\infty,\Omega}$.

Let $\Pi_h$ denote the interpolation operator which gives an elementwise constant function, in which the value in each element is the integrated average of the original function, i.e.

$$\Pi_h \rho|_{\Omega_{jk}} = \frac{1}{h^2} \int_{\Omega_{jk}} \rho, \quad \forall j, k$$

It is easily seen that $\int \Pi_h \rho = V$ and $\underline{\rho} \leqslant \Pi_h \rho \leqslant 1$ for any $\rho \in \mathscr{H}$. We verify (12) for $\Pi_h \rho$. Let, for the time being, $\rho_{jk}$ denote the value of $\Pi_h \rho$ in $\Omega_{jk}$. Then, denoting the unit vector in the

 

$x_1$-direction in $\mathbb{R}^2$ by $\mathbf{e}_1$, we have

$$|\rho_{j+1,k} - \rho_{jk}| = \frac{1}{h^2}\left|\int_{\Omega_{j+1,k}} \rho - \int_{\Omega_{jk}} \rho\right| = \frac{1}{h^2}\left|\int_{\Omega_{jk}} (\rho(\mathbf{x} + h\mathbf{e}_1) - \rho(\mathbf{x}))\,\mathrm{d}x\right|$$

$$\leqslant \frac{1}{h^2}\int_{\Omega_{jk}} |\rho(\mathbf{x} + h\mathbf{e}_1) - \rho(\mathbf{x})|\,\mathrm{d}x \leqslant \frac{c}{h^2}\int_{\Omega_{jk}} h = ch$$

Dealing with (13) similarly, we conclude that $\Pi_h$ maps $\mathscr{H}$ into $\mathscr{H}_h$. It remains to show that $\Pi_h\rho$ converges to $\rho$ uniformly as $h \to 0^+$.

Let $\mathbf{x}$ be arbitrary in $\Omega$. This point belongs to some $\overline{\Omega}_{jk}$. Since $\rho$ is continuous and $\overline{\Omega}_{jk}$ is connected and compact, $\rho$ attains all values between the maximum and minimum on $\overline{\Omega}_{jk}$. This means that there exists a $\mathbf{y} \in \overline{\Omega}_{jk}$ such that $\rho(\mathbf{y}) = \Pi_h\rho(\mathbf{x})$. Therefore,

$$|\Pi_h\rho(\mathbf{x}) - \rho(\mathbf{x})| = |\rho(\mathbf{y}) - \rho(\mathbf{x})| \leqslant c\sqrt{2}|\mathbf{y} - \mathbf{x}| \leqslant 2ch$$

which means that $\Pi_h\rho$ converges to $\rho$ uniformly as $h \to 0^+$.

*4.2.5. Optimality for a pair of cluster points.* In order to prove that any pair of cluster points $(\mathbf{u}^*, \rho^*)$, to a sequence of solutions to $(\mathrm{MC})_h$, that satisfies (18), is indeed solving (MC), we will verify

$$\ell(\mathbf{u}^*) \leqslant \ell(\mathbf{u}) \tag{23}$$

in which $(\mathbf{u}, \rho)$ is any admissible pair in (MC).

From Section 4.2.4 we have elements $\rho_h \in \mathscr{H}_h$ that converge uniformly to $\rho$. Let $\mathbf{u}_h$ be the solution to (14) for this $\rho_h$. Since $(\mathbf{u}_h, \rho_h)$ is an admissible pair in $(\mathrm{MC})_h$ we have

$$\ell(\mathbf{u}_h^*) \leqslant \ell(\mathbf{u}_h) \tag{24}$$

From Section 4.2.1 we get an element $\overline{\mathbf{u}} \in \mathbf{V}$ such that $\mathbf{u}_h \to \overline{\mathbf{u}}$ weakly in $\mathbf{V}$ for some subsequence. Section 4.2.2 gives that $\overline{\mathbf{u}}$ solves equilibrium for $\rho$, as well as $\mathbf{u}$ by assumption. Unambiguity hence yields $\mathbf{u} = \overline{\mathbf{u}}$.

Passing to the limit in (24) (for an appropriate subsequence), one arrives at (23), the desired result. The proof of the main conjecture, stated in the introduction of Section 4.2, is hereby complete.

## 5. NUMERICAL PROCEDURE

### *5.1. Description of the algorithm*

The optimization problem $(\mathrm{MC})_h$ with $\eta(\rho) = \rho^5$ is solved using computational procedures known from topology optimization (see Reference 14 for an overview). As the optimization problem is non-linear, it is solved by an iterative procedure where each step consists of a finite element analysis based on the current value of the design variables $\boldsymbol{\rho}$ (the element-wise constant values of the function $\rho_h$), followed by a change in design variables $\Delta\boldsymbol{\rho}$. For compliance optimization problems with only one (volume) constraint, the optimal change in design variables is mostly determined using optimality criteria algorithms due to their computational efficiency. However, in

 

this paper, with $2(n_x-1)(n_y-1)$ additional constraints, the optimal change in design variables must be determined with a different optimization algorithm. Here, we use the (sequential) linear programming (SLP) algorithm.

We solve the discretized compliance minimization problem $(\mathrm{MC})_h$ using a nested approach. The first part of the nested approach consists in a finite element analysis solving the equilibrium problem

$$\mathbf{K}(\boldsymbol{\rho})\mathbf{u}(\boldsymbol{\rho})=\mathbf{f} \tag{25}$$

where $\mathbf{f}$ is the force vector (assumed to be design independent) and $\mathbf{u}(\boldsymbol{\rho})$ is the displacement vector (representing the nodal values of the function $\mathbf{u}_h$). $\mathbf{K}(\boldsymbol{\rho})$ is the finite element stiffness matrix, assembled from the element stiffness matrices $\mathbf{K}_{jk}(\rho_{jk})=\rho_{jk}^p\mathbf{K}_0$ in the usual way. $\mathbf{K}_0$ is the element 8 by 8 stiffness matrix for a four node bilinear finite element consisting of solid material. The element stiffness matrix has only to be calculated once due to the regularity of the design domain (all elements are geometrically equivalent) and it is found as the integral $\mathbf{K}_0=\int \mathbf{B}^{\mathrm{T}}\mathbf{E}\,\mathbf{B}\,\mathrm{d}x$ where $\mathbf{B}$ is the usual strain–displacement matrix for four-node bilinear finite elements and $\mathbf{E}$ is the constitutive matrix under plane stress assumption.

The second part of the nested approach consists in solving the optimization problem

$$\begin{aligned}
\underset{\boldsymbol{\rho}}{\text{Minimize}}\quad & \Phi(\boldsymbol{\rho})=\mathbf{f}^{\mathrm{T}}\mathbf{u}(\boldsymbol{\rho})=\mathbf{u}(\boldsymbol{\rho})^{\mathrm{T}}\mathbf{K}(\boldsymbol{\rho})\mathbf{u}(\boldsymbol{\rho})=\sum_{jk}\rho_{jk}^p\mathbf{u}_{jk}(\boldsymbol{\rho})^{\mathrm{T}}\mathbf{K_0}\mathbf{u}_{jk}(\boldsymbol{\rho})\\
\text{subject to}\quad & -ch\leqslant\rho_{j+1,k}-\rho_{jk}\leqslant ch,\quad j=1,\ldots,n_x-1,\ k=1,\ldots,n_y\\
& -ch\leqslant\rho_{j,k+1}-\rho_{jk}\leqslant ch,\quad j=1,\ldots,n_x,\qquad k=1,\ldots,n_y-1\\
& \mathbf{a}^{\mathrm{T}}\boldsymbol{\rho}=V\\
& \underline{\boldsymbol{\rho}}\leqslant\boldsymbol{\rho}\leqslant\mathbf{1}
\end{aligned}$$

where $\mathbf{u}_{jk}(\boldsymbol{\rho})$ is the part of the global displacement vector $\mathbf{u}(\boldsymbol{\rho})$ which is associated with element $jk$ and $\boldsymbol{\rho}$, $\underline{\boldsymbol{\rho}}$, $\mathbf{1}$ and $\mathbf{a}$ are $N$-vectors and denote the value of the density variables, the minimum value of densities (non-zero to avoid singularity), the maximum values of densities and the area of the elements, respectively. It is noted that the first two lines among the side constraints are the 'new' constraints that represent the chosen design set restriction.

The above optimization problem is linearized in terms of $\boldsymbol{\rho}$ using the first part of a Taylor series expansion. Thereby, the optimal change in design variables $\Delta\boldsymbol{\rho}$, is determined by solving the linearized subproblem

$$\begin{aligned}
\underset{\Delta\boldsymbol{\rho}}{\text{Minimize}}\quad & \left\{\frac{\partial\Phi(\boldsymbol{\rho})}{\partial\boldsymbol{\rho}}\right\}^{\mathrm{T}}\Delta\boldsymbol{\rho}\\
\text{subject to}\quad & -ch-\rho_{j+1,k}+\rho_{jk}\leqslant\Delta\rho_{j+1,k}-\Delta\rho_{jk}\leqslant ch-\rho_{j+1,k}+\rho_{jk},\\
& \quad j=1,\ldots,n_x-1,\quad k=1,\ldots,n_y\\
& -ch-\rho_{j,k+1}+\rho_{jk}\leqslant\Delta\rho_{j,k+1}-\Delta\rho_{jk}\leqslant ch-\rho_{j,k+1}+\rho_{jk},\\
& \quad j=1,\ldots,n_x,\quad k=1,\ldots,n_y-1\\
& \mathbf{a}^{\mathrm{T}}\Delta\boldsymbol{\rho}=0\\
& \Delta\boldsymbol{\rho}_{\min}\leqslant\Delta\boldsymbol{\rho}\leqslant\Delta\boldsymbol{\rho}_{\max}
\end{aligned}$$

 

where $\Delta\boldsymbol{\rho}_{\min}$ and $\Delta\boldsymbol{\rho}_{\max}$ are move limits on the design variables and $\boldsymbol{\rho}$ is the current iterate. The move limits are adjusted for the box constraints of the original optimization problem. Again assuming design independent loads, the sensitivity of the objective function (compliance) with respect to a change in design variable $\rho_{jk}$ is found as

$$\frac{\partial\Phi(\boldsymbol{\rho})}{\partial\rho_{jk}} = 2\left\{\frac{\partial\mathbf{u}(\boldsymbol{\rho})}{\partial\rho_{jk}}\right\}^{\mathrm{T}}\mathbf{K}(\boldsymbol{\rho})\mathbf{u}(\boldsymbol{\rho}) + \mathbf{u}(\boldsymbol{\rho})^{\mathrm{T}}\frac{\partial\mathbf{K}(\boldsymbol{\rho})}{\partial\rho_{jk}}\mathbf{u}(\boldsymbol{\rho})$$
$$= -\mathbf{u}(\boldsymbol{\rho})^{\mathrm{T}}\frac{\partial\mathbf{K}(\boldsymbol{\rho})}{\partial\rho_{jk}}\mathbf{u}(\boldsymbol{\rho}) = -p\rho_{jk}^{(p-1)}\mathbf{u}_{jk}(\boldsymbol{\rho})^{\mathrm{T}}\mathbf{K_0}\mathbf{u}_{jk}(\boldsymbol{\rho}) \tag{26}$$

where it was used that

$$\mathbf{K}(\boldsymbol{\rho})\frac{\partial\mathbf{u}(\boldsymbol{\rho})}{\partial\rho_{jk}} = -\frac{\partial\mathbf{K}(\boldsymbol{\rho})}{\partial\rho_{jk}}\mathbf{u}(\boldsymbol{\rho}) \tag{27}$$

which comes from the differentiation of the equilibrium equation (25).

Since the linear programming problem defined above is very sparse, it can be solved efficiently using the sparse linear programming solver DSPLP[16] from the SLATEC library.

The move limit strategy is important for the stable convergence of the algorithm. Here, we use a global move limit strategy, where the move limit for all design variables is increased by a factor of 1·05 if the change in the cost function between two steps is negative. Similarly the move limit is decreased by a factor of 0·9 if the change in the cost function is positive.

Because of the non-convexity of the design problem, starting the optimization algorithm with a high value of the penalty parameter $p$ often results in the algorithm converging to a local minimum. Therefore, we use a *continuation method*, i.e. we start with a low value $p = 1$, we let the procedure converge, then we increase $p$ with 0·5, in turn letting the algorithm converge, and continue this until $p$ equals 5.

### 5.2. Numerical examples and discussion

To demonstrate the method, we consider the optimal topological design of the so-called MBB-beam[17] shown in Figure 1. As we are only considering qualitative results in this paper, the material data and dimensions for the problem are chosen non-dimensional. The load is applied as a constant line load and the beam is line-supported at the lower left and right edges. The base material has Young's modulus 1·0 and Poisson's ratio 0·3 and the minimum density constraint is $\underline{\rho} = 0{\cdot}01$. The material is allowed to fill 50 per cent of the design domain. The design problem is solved for different mesh sizes $h$ and different values of the slope constraint $c$.

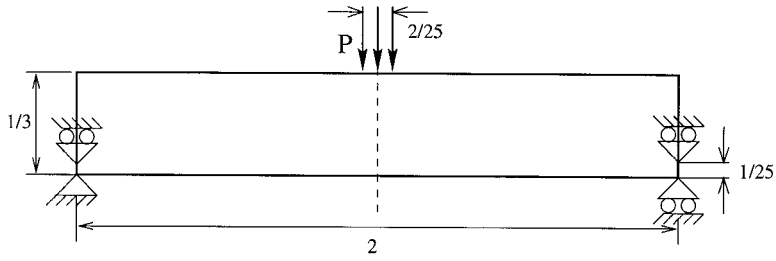


Figure 1. Geometry and load-case for the considered design problem

 

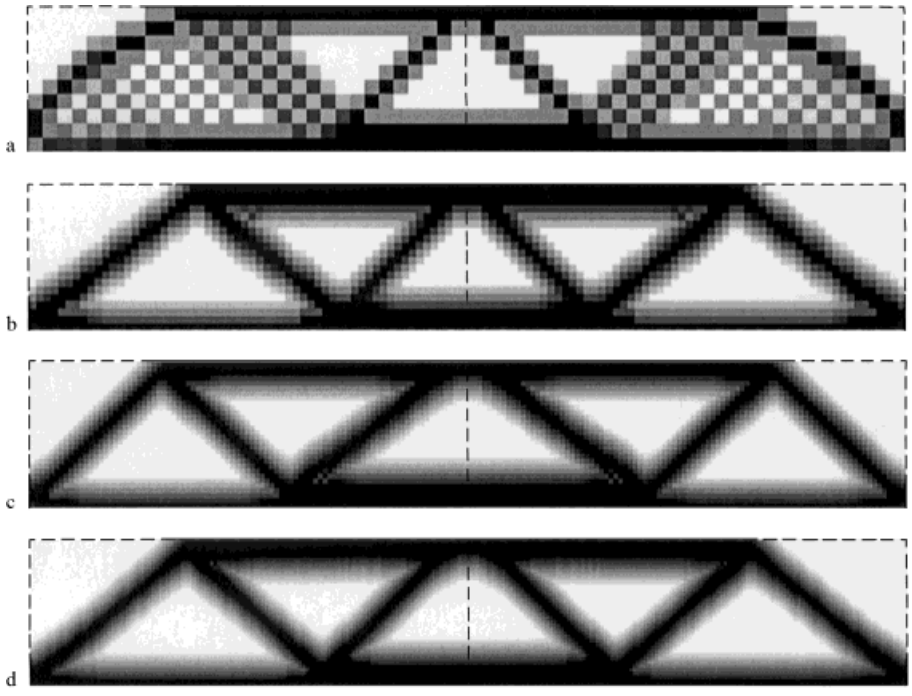


Figure 2. Optimal designs for fixed $c = 15$ and varying mesh size, $h = 1/30$, $1/60$, $1/90$ and $1/120$ (from top to bottom)

Because of the use of the continuation method for the increase of the penalty parameter, the algorithm requires as many as 300 iterations to converge. Furthermore, solving the LP problem is very time-demanding because of the large number of constraints. For the considered examples, the increase in computational time lies between a factor of 100 and 1000 compared to compliance optimization problems without slope constraints.

Figure 2 shows the resulting topologies for fixed $c = 15$ and varying discretizations. It can be seen that the topologies are independent of the discretization. The actual values of the compliance for the three solutions are seen in Table I.

Figure 3 shows the resulting topologies for fixed $c = 23$, varying discretizations and *point support and load*. Again, the actual values for the compliances are seen in Table I.

In case one runs into (what seems to be) problems with numerical results, one should keep in mind that, since we have established a convergence proof, such problems are necessarily of at least one of the following three kinds: (I) one has not a sufficiently small $h$ for the FE solution to be close to an exact solution, (II) the algorithm does not manage to solve the problem $(\mathrm{MC})_h$ and (III) consecutive discrete solutions for different meshes might approximate two *different* true solutions. The category (II) is quite possible since $(\mathrm{MC})_h$ is non-convex, and the objective function is very flat with respect to some design changes. In category (I) one is simply left with the option to solve $(\mathrm{MC})_h$ for a finer mesh, and (III) is actually not a problem, just a possible event to keep in mind.

Figure 4 shows resulting topologies for a fixed mesh of $90 \times 30$ elements and different values of $c$. From the figure, we can see that it is possible to control the complexity (and thereby the

 

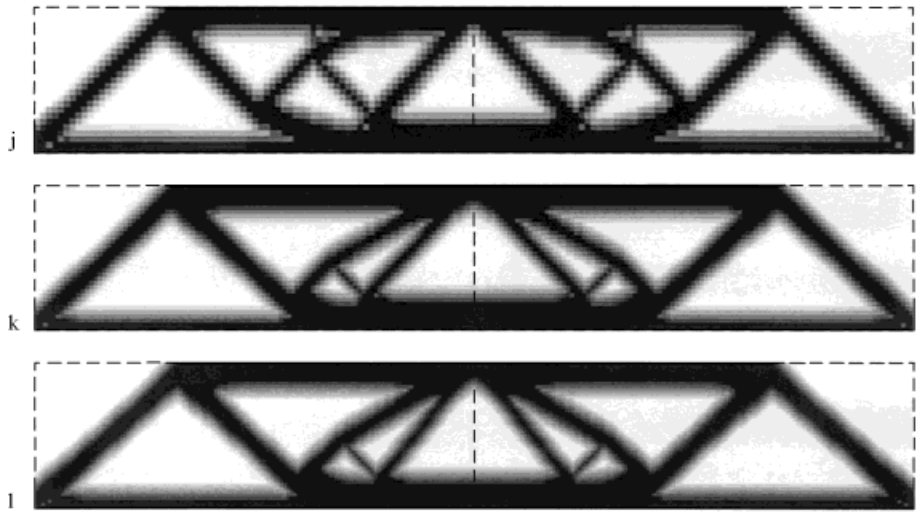


Figure 3. Optimal designs for fixed $c = 23$ and varying mesh size, $h = 1/75$, $1/105$ and $1/135$ (from top to bottom)

Table I. Data for the examples

| Example | $n_x \cdot n_y = N$ | $h$ | $c$ | $hc$ | $\Phi$ |
|---|---|---|---|---|---|
| a | $30 \cdot 10 = 300$ | 1/30 | 15 | 0·50 | 329·4 |
| b | $60 \cdot 20 = 1200$ | 1/60 | 15 | 0·25 | 281·8 |
| c | $90 \cdot 30 = 2700$ | 1/90 | 15 | 0·17 | 284·3 |
| d | $120 \cdot 40 = 4800$ | 1/120 | 15 | 0·13 | 282·2 |
| e | $90 \cdot 30 = 2700$ | 1/90 | 60 | 0·67 | 248·6 |
| f | $90 \cdot 30 = 2700$ | 1/90 | 45 | 0·50 | 221·0 |
| g | $90 \cdot 30 = 2700$ | 1/90 | 20 | 0·22 | 261·8 |
| h | $90 \cdot 30 = 2700$ | 1/90 | 15 | 0·17 | 284·3 |
| i | $90 \cdot 30 = 2700$ | 1/90 | 5 | 0·06 | 809·6 |
| j | $75 \cdot 25 = 1875$ | 1/75 | 23 | 0·31 | 255·4 |
| k | $105 \cdot 35 = 3675$ | 1/105 | 23 | 0·22 | 258·6 |
| l | $135 \cdot 45 = 6075$ | 1/135 | 23 | 0·17 | 260·0 |
| m | $30 \cdot 10 = 300$ | 1/30 | 15 | 0·50 | 297·8 |

manufacturability) of the optimal design by choosing different values of $c$. A larger $c$ allows for more 'bars' and a low one yields a small number of wide 'bars' (however with grey zones).

Some (intermediate) values of $\rho^*$ might be poorly approximated with a 'jagged field' in $\rho_h^*$ for large $h$. However, these instabilities, such as checkerboard patterns, can be made arbitrarily weak by decreasing $h$.

Figure 5 shows that using nine-node biquadratic finite elements helps in producing checkerboard free designs. The topology in Figure 5 should be compared with the topology a in Figure 2. As the use of nine-node elements implies that the computational time is increased dramatically (up to a factor of 16) their use is considered impractical for general topology design problems.

 

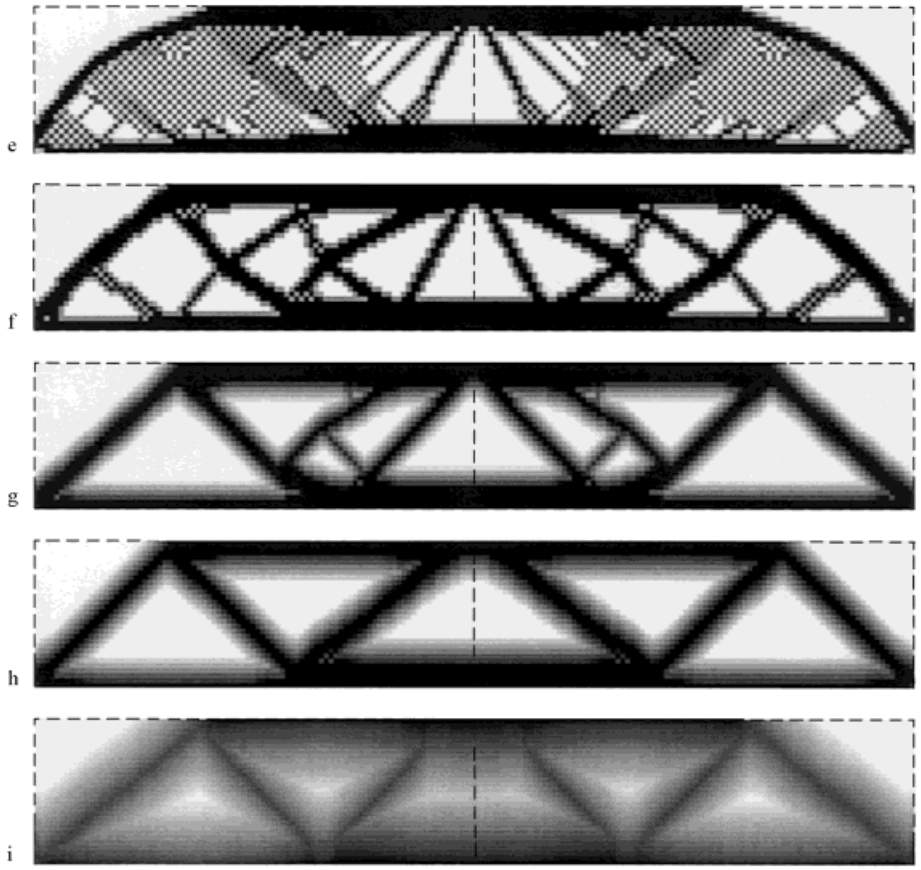


Figure 4. Optimal topologies for varying $c = 60$, 45, 20, 15 and 5 (from top to bottom), and fixed mesh $h = 1/90$

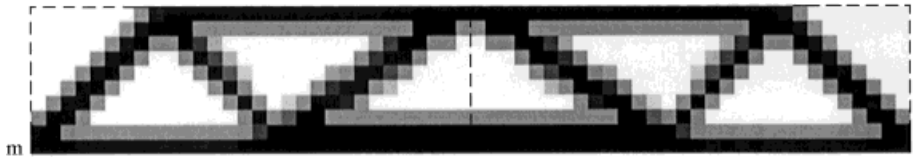


Figure 5. Optimal design using nine node elements, $c = 15$ and mesh size $h = 1/30$

### 5.3. *Conclusions*

In this paper we have furnished a traditional continuum topology optimization problem with an extra design constraint. This constraint — an upper bound ($c$) on the maximum slope—makes the problem well-posed in the sense that existence of solutions is guaranteed, and the solutions obtained by a finite element method will converge uniformly to the set of exact solutions as the mesh is refined. The constant $c$ allows for a control of the maximum structural complexity and hence the manufacturability. A larger $c$ permits a larger number of holes. Given a desired

 

complexity, i.e. a given $c$, one can estimate *a priori* the required number of elements: We suggest, partly based on the data in Table I, that $hc$ should be kept below $1/3$ as a rule of thumb in order to obtain designs with no, or very minor, checkerboard patterns.

The proposed approach is mathematically rigorous and hence provides 'mesh-independent' designs. However, the computational cost is extremely high. A heuristic method based on image processing techniques, which was proposed by Sigmund[11, 12] *seems* to give similar topological designs with much less computational effort.

## APPENDIX

### *Compactness of* $\mathscr{H}$

Crucial for the existence of solutions to (MC), as well as for the relation between (MC) and its discretized version $(\mathrm{MC})_h$, is the compactness of the design set that follows from the slope constraints.

Let $\{\rho_m\}$ be any sequence in $\mathscr{H}$. The compactness of $\mathscr{H}$ in $C^0(\overline{\Omega})$ means that there exists a subsequence (denoted with the same notation) and an element $\rho \in \mathscr{H}$, such that $\rho_m \to \rho$ uniformly in $\Omega$. Even though this is well known to a mathematical society, we next proceed to prove this conjecture because of its extreme relevance to the present paper.

The inclusion of $W^{1,\infty}(\Omega)$ into $C^0(\overline{\Omega})$ is compact due to Sobolev's imbedding theorem, see e.g. Reference 13, which means that there is a subsequence, denoted $\{\rho_m\}$ again, and an element $\rho \in C^0(\overline{\Omega})$ such that $\{\rho_m\}$ converges uniformly to $\rho$. One easily concludes that $\underline{\rho} \leqslant \rho \leqslant 1$ and $\int \rho = V$. It remains to show that the first derivatives exist in $L^\infty(\Omega)$ and are bounded by $c$ almost everywhere in $\Omega$.

From the definition of weak derivative we have, for $i = 1, 2$,

$$\int \frac{\partial \rho_m}{\partial x_i} \varphi = -\int \rho_m \frac{\partial \varphi}{\partial x_i}, \quad \forall \varphi \in \mathscr{D} \tag{28}$$

The sequences $\{\partial \rho_m / \partial x_i\}$ are bounded in $L^\infty(\Omega)$, and so, by Banach–Alaoglu's theorem, see e.g. Reference 18, there are elements $h_i \in L^\infty(\Omega)$ such that $|h_i| \leqslant c$ and, at least for some subsequence,

$$\int \frac{\partial \rho_m}{\partial x_i} \varphi \to \int \varphi h_i, \quad \forall \varphi \in L^1(\Omega) \tag{29}$$

We finally show that the $h_i$'s are the weak derivatives of $\rho$. For any $\varphi \in \mathscr{D}$ we certainly have

$$\int \rho_m \frac{\partial \varphi}{\partial x_i} \to \int \rho \frac{\partial \varphi}{\partial x_i}$$

which with (28) and (29) gives

$$\int \varphi h_i = -\int \rho \frac{\partial \varphi}{\partial x_i}$$

i.e. $h_i = \partial \rho / \partial x_i$.

 

ACKNOWLEDGEMENTS

The authors are indebted to Martin P. Bendsøe, Department of Mathematics, Technical University of Denmark, for inspiration and valuable comments on the present work.

This work was financially supported by the Swedish Research Council for Engineering Sciences (TFR) and Denmark's Technical Research Council (Programme of Research on Computer-Aided Design).

REFERENCES

1. M. P. Rossow and J. E. Taylor, 'A finite element method for the optimal design of variable thickness sheets', *AIAA J.*, **11,** 1566–1568 (1973).
2. H. P. Mlejnek and R. Schirrmacher, 'An engineering approach to optimal material distribution and shape finding', *Comput. Meth. Appl. Mech. Engng.*, **106,** 1–26 (1993).
3. M. P. Bendsøe and N. Kikuchi, 'Generating optimal topologies in structural design using a homogenization method', *Comput. Meth. Appl. Mech. Engng.*, **71,** 197–224 (1988).
4. L. Ambrosio and G. Buttazzo, 'An optimal design problem with perimeter penalization', *Calc. Var.*, **1,** 55–69 (1993).
5. R. B. Haber, M. P. Bendsøe and C. Jog, 'A new approach to variable-topology shape design using a constraint on the perimeter', *Struct. Optim.*, **11,** 1–12 (1996).
6. M. P. Bendsøe, J. M. Guedes, R. B. Haber, P. Pedersen and J. E. Taylor, 'An analytical model to predict optimal material properties in the context of optimal structural design', *J. Appl. Mech.*, **61,** 930–937 (1994).
7. F. I. Niordson, 'Optimal design of plates with a constraint on the slope of the thickness function', *Int. J. Solids Struct.*, **19,** 141–151 (1983).
8. M. P. Bendsøe, 'On obtaining a solution to optimization problems for solid, elastic plates by restriction of the design space', *Int. J. Struct. Mech.*, **11,** 501–521 (1983).
9. I. Hlaváček, I. Bock and J. Lovišek, 'Optimal control of a variational inequality with applications to structural analysis. II. Local optimization of the stress in a beam III. Optimal design of an elastic plate', *Appl. Math. Optim.*, **13,** 117–136 (1985).
10. J. Petersson, 'A finite element analysis of optimal variable thickness sheets', preprint, Department of Mathematics, Technical University of Denmark, 2800 Lyngby, Denmark, 1996.
11. O. Sigmund, 'Design of Material Structures Using Topology Optimization', *Ph.D. Thesis*, Department of Solid Mechanics, Technical University of Denmark, 1994.
12. O. Sigmund, 'On the design of compliant mechanisms using topology optimization', *Mech. Struct. Mach.*, **25,** to appear.
13. R. A. Adams, *Sobolev Spaces*, Academic Press, New York, 1975.
14. M. P. Bendsøe, *Optimization of Structural Topology, Shape, and Material*, Springer, Berlin, 1995.
15. P. G. Ciarlet, *The Finite Element Method for Elliptic Problems*, North-Holland, Amsterdam, 1978.
16. R. J. Hanson and K. L. Hiebert, 'A sparse linear programming subprogram', *Technical Report SAND81–0297*, Sandia National Laboratories, 1981.
17. N. Olhoff, M. P. Bendsøe and J. Rasmussen, 'On CAD-integrated structural topology and design optimization', *Comput. Meth. Appl. Mech. Engng.*, **89,** 259–279 (1992).
18. W. Rudin, *Functional Analysis*, McGraw-Hill, New York, 1973.

 